Energetic Materials Frontiers 2 (2021) 51–61

Contents lists available at ScienceDirect

Energetic Materials Frontiers

journal homepage: www.keaipublishing.com/en/journals/energetic-materials-frontiers

Solubility behaviour of CL-20 and HMX in organic solvents and solvates of CL-20

Dirk Herrmannsdörfer [a,*], Jörg Stierstorfer [b], Thomas M. Klapötke [b]

[a] Fraunhofer Institute for Chemical Technology ICT, Joseph-von-Fraunhofer-Str. 7, 76327, Pfinztal, Germany
[b] Department of Chemistry Energetic Materials Research, Ludwig-Maximilians University of Munich, Butenandtstr 5 - 13 (Haus D), 81377, Munich, Germany

ARTICLE INFO

Keywords:
CL-20
Cocrystal
Conformation
Energetic material
HMX
Solubility
Solvate

ABSTRACT

2,4,6,8,10,12-Hexanitro-2,4,6,8,10,12-hexaazaisowurtzitane (CL-20) and 1,3,5,7-tetranitro-1,3,5,7-tetrazoctane (HMX) are promising cocrystal coformers, but only little solubility data are available. Knowledge about their solubility and solvate formation is essential for the development of cocrystallisation experiments. This paper provides the solubility values of HMX and CL-20 in 29 solvents at 293.15 K and 333.15 K as well as the solubility in five 2-propanol solvent mixtures at 293.15 K. Novel CL-20 solvates of 5-methyloxolan-2-one, 1,3-dioxolan-2-one, tetrahydrotiophene 1-oxide, 1,3-dioxolane, furan-2-carbaldehyde and butane-2,3-dione have been isolated and characterised. For all new solvates, single crystal data were obtained, except for furan-2-carbaldehyde. The novel ϑ-conformation of CL-20 was observed in the tetrahydrotiophene 1-oxide solvate. It was found that none of the tested solvents and likely no existing solvent exhibits a beneficial solubility ratio of CL-20 and HMX in the tested temperature range, exceptionally good solubility ratios are most likely the result of solvate formation, and that solvate forming solvents cannot be categorically excluded from consideration as solvent for cocrystallisation of HMX and CL-20.

1. Introduction

The CL-20/HMX cocrystal is one of the most promising energetic cocrystals due to its reported reduced impact sensitivity compared to CL-20 and the improved detonation properties compared to HMX.[1] A multitude of cocrystallisation methods have been described in literature for this cocrystal. For some of the reported methods, such as spray drying[2] or liquid-assisted grinding,[1,3,4] the solubility of the individual cocrystal former is of lesser importance. For solution-based cocrystallisation techniques, such as solvent evaporation,[1,5,6] antisolvent crystallisation,[3,7] reaction cocrystallisation,[7] and cooling crystallisation,[7] however, detailed knowledge of the size and position of the cocrystal phase region in the corresponding phase diagram is required for the design of a reproducible and efficient crystallisation method. As the full determinations of the phase diagrams are very time consuming, solubility data of CL-20 and HMX in the respective solvent might be used to assess a solvent's suitability. Further factors influence the suitability of a solvent such as chemical incompatibility and solvate formation. It has been reported that solvate formation can hinder cocrystallisation.[8] The aim of this study, therefore, was to identify a solvent that exhibits a beneficial solubility ratio, but does not form solvates with either CL-20 or HMX. In this paper we present the solubility data of CL-20 and HMX in 29 solvents at 293.15 K and 333.15 K as well as in selected solvent mixtures. Furthermore, six novel solvates of CL-20 are described and the single crystal structures of five of them discussed. This includes the discussion of the novel ϑ-conformation of CL-20.

2. Experimental section

Table 1 displays the purity and supplier of the utilised solvents. All solvents were used without further purification and stored over 3 Å molecular sieve if used repeatedly. ε-CL-20 (lot number 573S98) was obtained from SNPE. The chemical purity was determined *via* ^{1}H NMR and HPLC to be 98.3 and 99.4%, respectively. Further analysis details are found in the supporting information. β-HMX (lot number NSI 00E 000 E004) was purchased from Chemring Nobel. The chemical purity has been determined *via* ^{1}H NMR and HPLC to be 98.7 and 99.3%, respectively. Further analysis details are found in the supporting information.

* Corresponding author.
E-mail address: dirk.herrmannsdoerfer@ict.fraunhofer.de (D. Herrmannsdörfer).

https://doi.org/10.1016/j.enmf.2021.01.004
Received 18 December 2020; Received in revised form 7 January 2021; Accepted 13 January 2021
Available online 11 February 2021

Table 1
Description of materials used in this paper.

solvent	Source	Purity /%	Designation
2,4,6,8,10,12-Hexanitrohexaazaisowurtzitan	SNPE	98.9[a]	CL-20
Cyclotetramethylentetranitramin	Chemring Nobel	99.0[a]	HMX
Tetrahydro-2H-pyran-2-one	Sigma-Aldrich	≥97.5[b]	**2**
5-Methyloxolan-2-one	Sigma-Aldrich	99[b]	**3**
Cyclopentanone	Merck	99[b]	**4**
4-Methyloxetan-2-one	Sigma-Aldrich	98[b]	**5**
Oxolane	Th.Geyer	≥99.9[b]	**6**
1,3-Dioxolan-2-one	Aldrich	98[b]	**7**
2-Oxepanone	Sigma-Aldrich	98[b]	**9**
Ethyl acetate	VWR	99[b]	**10**
5-Ethyloxolan-2-one	Sigma-Aldrich	≥98[c]	**11**
Cyclohexanone	Sigma-Aldrich	99.5[b]	**12**
Tetrahydrotiophene-1-oxide	Sigma-Aldrich	96[b]	**13**
Propan-2-one	VWR	100[b]	**14**
Thiophene	Sigma-Aldrich	≥99[b]	**15**
Furan	Sigma-Aldrich	≥99[b]	**16**
1,3-Dioxolane	Sigma-Aldrich	99[b]	**17**
4-Methyl-1,3-dioxolan-2-one	Roth	99.7[b]	**18**
Methoxysulfinyloxymethane	Sigma-Aldrich	99[b]	**19**
N-Cyclohexyl-2-pyrrolidone	Sigma-Aldrich	99[b]	**20**
3-Methylbutyl acetate	Honeywell	98[b]	**21**
5-Propyloxolan-2-one	Sigma-Aldrich	≥98[b]	**22**
Diethyl carbonate	Sigma-Aldrich	≥99[b]	**23**
Ethyl methyl carbonate	Sigma-Aldrich	98[b]	**24**
Dimethyl carbonate	Sigma-Aldrich	≥99[b]	**25**
Tetramethylurea	Sigma-Aldrich	99[b]	**26**
Formic acid	Sigma-Aldrich	≥95[b]	**27**
Acetonitrile	Fisher Scientific	≥99[b]	**29**
2-Propanole	Roth	99.8[b]	**30**
2-Methylpropanenitrile	Sigma-Aldrich	99[b]	**31**
Nitromethane	LD sportsline	99.9[b]	**32**
Butane-2,3-dione	Sigma-Aldrich	97[b]	**33**

[a] Determined via ^{1}H NMR and HPLC.
[b] Provided by suppliers.

2.1. Characterisation methods

Sample mass was determined using a Kern 770 analytical balance (accuracy 0.1 mg).

Raman spectra were obtained with a Bruker RFS 100/S Raman spectrometer equipped with a 1064 nm ND:YAG-laser operated at 450 mW and a liquid-nitrogen-cooled germanium-detector. The spectra were obtained between 80 and 3500 cm^{-1} with a spectral resolution of 1 cm^{-1}. 75 scans were accumulated.

For the x-ray diffraction of all compounds, an Oxford Xcalibur3 diffractometer with a CCD area detector was employed for data collection using Mo-Kα radiation (λ = 0.71073 Å). By using the CRYSALISPRO software[9] the data collection and reduction were performed. The structures were solved by direct methods (SIR92,[10] SIR - 97[11,12] or SHELXS-97[13,14]) and refined by full-matrix least-squares on F2 (SHELXL[13,14]) and finally checked using the PLATON software[15] integrated in the WinGX software suite. Non-hydrogen atoms were refined anisotropically and the hydrogen atoms were located and freely refined. The absorptions were corrected by a SCALE3ABSPACKmultiscan method.[16]

DSC analysis was carried out using a TA Instruments DSC Q2000 V24.10 build 122. Samples were heated from 298 up to 543 K at the rate of 5 $K \cdot min^{-1}$ in a hermetically sealed aluminium pan. The sample quantity in all experiments was between 0.5 and 1.5 mg.

TGA was carried out using a TA Instruments TGA Q5000 V3.15 build 263. Samples were heated from 298 up to 573 K at the rate of 5 $K \cdot min^{-1}$ in a platinum pan. The sample quantity in all experiments was between 0.9 and 4 mg.

2.2. Solubility determination

A moderate excess of HMX or CL-20 was placed in a 6 mL or 20 mL glass vessel. Depending on the expected solubility, between 0.5 g and 15 g solvent/solvent mixture were added. The solution was agitated at 800 rpm and tempered *via* a Ditabis MKR 23 thermo block mixer equipped with a matching thermo block for the reaction vessels. Typically, after 2 h and 4 h, the solid was sedimented and part of the clear solution removed by syringe. Enough solution was removed to ensure at least 10 mg evaporation residue. Directly after transfer, the solution mass was determined. The solvent was removed under vacuum and the mass of the remaining solid was determined. The remaining solid in the glass vessel was washed according to the standard washing procedure,[7] dried, and analysed *via* Raman spectroscopy. No phase change was detected, except for the solvates discussed later, and α-CL-20 that formed in **27** (total conversion at 293.15 K and 1/3 conversion at 333.15 K) and **25** (traces of α at 293.15 K). A solubility determination was considered successful if the two obtained values differed from one another by less than 5%. This relatively large error margin was chosen because comparison among literature shows that solubility data between different determination setups and especially different raw material varies often by more than 5%.[17] Furthermore, if the determined solubility was less than 0.003 $mol \cdot kg^{-1}$, or the difference in determined solubility was less than 0.001 $mol \cdot kg^{-1}$ the experiment was considered successful independent of the error between the obtained values because of the increase in error due to excessively low solubilities. This procedure was chosen even though it does not provide certainty whether the obtained solubility value truly represents the equilibrium solubility. It is typically preferred to perform an experiment in which the substance in question is dissolved at higher temperature and the solution is subsequently cooled down in addition to the described method.[18] In theory, this provides one with the certainty that the equilibration time was sufficient if the solubility values of both experiments concur. This method is, however, unsuitable for CL-20. For once CL-20 exhibits only a very weak temperature dependency of solubility. In addition, at different temperatures different CL-20 polymorphs can form. It is hence possible that at elevated temperature a polymorphic transformation process occurs which at lower temperature first has to be reversed to form the true equilibrium at this temperature. No solubility data were determined if due to solvate formation the solution completely solidified during the solubility determination. No solubility values have been determined for some solvate forming solvents for this reason. Additionally, no solubility data was determined for **28** and **33** because discolouration of the obtained solid occurred after the solvent was evaporated. Solubility values are calculated as molalities b_i according to the formula $b_i = \frac{m_i}{m_j \cdot M_i}$ where m_i represents the solute's mass, M_i represents the solute's molar mass, and m_j represents the solvent/solvent mixture mass. Solvent compositions are calculated as mass fractions w_j according to the formula $w_j = \frac{m_j}{m_j + m_k}$ where m_j and m_k represent the solvent masses.

HMX, CL-20, and their solvates are capable of mass explosion

initiated via static electricity, friction or impact. Appropriate care must be taken when handling these materials.

2.3. Preparation of solvates

The following procedure describes the basic course of action for producing the solvates. Because of specifics of the individual solvent, deviations from this procedure were undertaken.

4000 mg of the corresponding solvent were added to an appropriate amount of CL-20 to form a supersaturated solution in a 20 mL glass vessel. The slurry was agitated at 600 rpm at 293.15 K for **3**, **13**, **17** and **33** or 333.15 K for **7** and **28** until conversion occurred. Crystals for single crystal analysis were collected if initially high-quality crystals formed and were stored under mother liquor or Fomblin YR-1800 until measurement. 2000 mg CL-20 (4.56 mmol) were added to the reaction mixture over the course of 48 h to enforce the formation of larger crystals by keeping the supersaturation low. Larger and more defect lean crystals were preferred to facilitate solid-liquid separation. The reaction mixture was divided and the mother liquor of one half was removed *via* a syringe and filter paper. The solid was dried at room temperature and atmospheric pressure until constancy of mass was achieved. Raman analysis of the dried material was carried out. Raman, TGA, and DSC analysis were carried out with the other half of the collected solid. Here the solid was quickly washed following the standard washing procedure published elsewhere.[7] The washed solid was only briefly dried to ensure total evaporation of 2-propanol, but prevent excessive solvent evaporation.

3. Results and discussion

3.1. Solubility data

Most of the published solubility data for HMX and CL-20 are displayed in Table 2. Of the published solvents, oxolan-2-one (**1**) appears to possess the overall most suitable solubilities of CL-20 and HMX for generating the cocrystal. That is because for cocrystallisation the cocrystal phase region in the solvent must be considered. It is reasonable to assume that the position of the cocrystal phase region correlates with the solubilities of the individual coformers, as this holds true for other systems.[26] One can, therefore, assume that a solubility ratio of CL-20 to HMX of 2:1 would be most beneficial. The ratio 2:1 is proposed because the CL-20/HMX cocrystal is composed of two parts CL-20 per part HMX. Solvent **1** possesses at 333 K a solubility ratio of 2:1 based on the literature solubility data. Solvent **1**, however, also forms solvates not only with HMX,[27] but also with CL-20.[28] A solvents ability to form solvates can hinder cocrystal formation[8] because solvate formation is basically (depending on the preferred definition for cocrystal)[29–32] a competing cocrystallisation. In the ternary phase diagram of **1**, CL-20, and HMX would, therefore, coexist at least three cocrystal phase regions which most likely at least partially overlap. It was, hence, attempted to identify alternatives to **1** that also possess a solubility ratio close to 2:1, but do not form solvates. Because of the limited available data, **1** was chosen as the ancestral molecule from which most of the tested molecules are derived by successive exchange of functional groups or alkyl units (Fig. 1). The literature data indicate that the solubility of CL-20 is nearly temperature independent, whereas the HMX solubility increases with increasing temperature. Solubility determinations were, thus, carried out at 293.15 K and 333.15 K. The upper temperature was chosen as a compromise between the better solubility values for HMX at higher temperatures, safety concerns, and the limiting factor of boiling points. The obtained solubility data are displayed in Table 3.

To validate the method, two sets of obtained solubility data of CL-20 are compared to the corresponding measurement data of Cui et al.[20] The solubility values and deviations of measurement are shown in Table 4. The results indicate the validity of the solubility determination method.

Multiple effects of the solvent molecule structure and its functional groups on the solubilities are apparent. In most cases only the solubility of CL-20 can be discussed because the HMX solubility is often too low for changes in solubility to be significant in face of the experimental error. The strongest effect on the solubility of CL-20 and HMX in carbonyl compounds with at least one adjacent oxygen has the overall molecular geometry i.e. whether the carbonyl group is situated in a ring. This can most easily be seen in comparing the lactone **3** with the similar acetate **10**. This is the result of the prevalence of the (*Z*)-conformation over the (*E*)-conformation in noncyclic esters. The prevalence was attributed to a minimisation of dipole-dipole repulsion in the (*Z*)-conformation.[33–35] As a result, the overall dipole moment of the carboxyl group is weaker in noncyclic esters because in (*E*)-conformation the individual dipoles align, whereas in (*Z*)-conformation the opposing dipoles weaken the net dipole moment. As the dipole moment is one of the key factors in determining the solubility of CL-20,[36] (and presumably also HMX) it is very likely that the difference in dipole moments explains most of the difference in solubility between the tested cyclic and noncyclic esters. The same reasoning can also explain the lower solubilities in the noncyclic carbonates compared to **18**. On the same note, the CL-20 solubility in **2** most likely increases that significantly with increasing temperature because the less stable conformer has a higher dipole moment.[37] Increased mobility of the alkyl group is most likely responsible for the solubility

Table 2
Compilation of the available solubility data of CL-20 and HMX.

Solvent	CAS Nr.	b_{HMX}/mol • kg^{-1}		b_{CL-20}/mol • kg^{-1}	
		293-298 /K	323-333 /K	293-333 /K	323-333 /K
1-Methylpyrrolidin-2-one	872-50-4			2.533[19]; 2.622[20]	0.776[19]; 2.524[20]
2-Oxepanone	502-44-3	0.230[21]			
4-Methyl-1,3-dioxolan-2-one	108-32-7	0.069[22]	0.312[22]	1.426[19]	1.723[19]
5-Methyloxolan-2-one	108-29-2	0.311[21]			
Acetic acid	64-19-7	0.001[23]	0.003[23]		
Acetic anhydride	108-24-7		0.007[23]		
Acetonitrile	75-05-8	0.068[24]	0.147[23]	1.278[20]	1.997[20]
Butyl acetate	123-86-4			0.730[19]	0.662[19]
Cyclohexanone	108-94-1	0.034[24]	0.240[23]	1.912[20]	1.960[20]
Dimethyl sulfoxide	67-68-5	1.924[24]	2.296[24]; 1.594[23]		
Ethane-1,2-diol	107-21-1			0.022[17]	0.034[17]
Ethanol	64-17-5			0.014[17]; 0.005[19]	
Ethyl acetate	141-78-6			1.027[17]; 1.141[19]; 1.246[20]	0.808[20]
Hexamethylphosphoric triamide	680-31-9	0.047[24]			
Methyl acetate	79-20-9			1.209[19]	1.438[19]
N,N-Dimethylformamide	68-12-2		0.375[23]	1.506[19]; 1.476[20]	1.597[19]; 1.860[20]
Nonan-5-one	502-56-7			0.399[19]	0.338[19]
Oxolan-2-one	96-48-0	0.375[21]; 0.405[24]; 0.422[25]	0.641[25]	0.822[19]	1.296[19]
Pentan-3-one	96-22-0			1.209[19]	1.221[19]
Propan-2-one	67-64-1	0.095[24]; 0.081[23]		2.159[17]; 2.654[19]	
Tetrahydro-2H-pyran-2-one	542-28-9	0.219[21]			

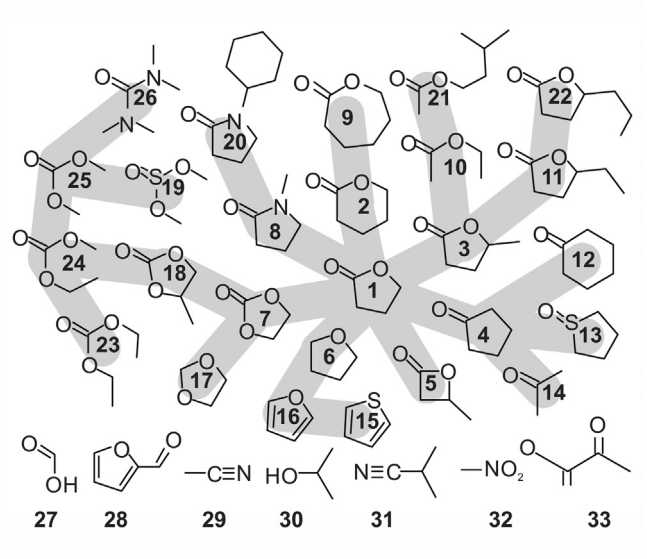

Fig. 1. Molecular structure of the utilised solvents. Grey branches visualise the relation of the molecules branching out from **1**. The molecules **27** to **33** have not been directly derived in this fashion.

reduction of CL-20 in **10** and **21**. Due to the rigid frame of **32** conformational changes, however, cannot explain the significant increase in solubility of CL-20. Also, the solubility increase of CL-20 in **18** is antithetic to the expected reduction in effective dipole moment of **18** with increasing temperature. The solubility changes of CL-20 were typically the result of dipole moment changes of the solvents with temperature increase. This indicates that CL-20 per se does not exhibit a temperature dependent solubility. In contrast, HMX shows a pronounced increase in solubility with increasing temperature in all tested solvents. Because of the often low HMX solubility in the solvents that exhibited significant CL-20 solubility changes with temperature, no correlation of the HMX solubility to changes in solvent dipole moment can be discerned. On average, the solubility of HMX doubled by increasing the temperature from 293.15 K to 333.15 K. The smallest increase exhibits **20** with an increase of 12% whereas the solubility in **26** almost triples. Of the tested solvents, **13** exhibits at 333.15 K and 293.15 K by far the highest solubility of HMX. The solubility is only surpassed by dimethyl sulfoxide.[23,24]

Of the tested solvents, **26** and **17** exhibited a slow decomposition of CL-20 in solution both at 293.15 K and 333.15 K. It is documented that CL-20 is chemically incompatible with amines.[38] Solvent **20,** a lactam, did not show signs of chemical incompatibility. Apparently, the reported incompatibility also encompasses amides, but potentially not lactams. The observed incompatibility of CL-20 with **17** is likely the result of a high HOMO-energy or a low ionisation potential of **17**, as Thome[36] found an unusually high CL-20 solubility for the chemically similar solvent 2, 2'-[ethane-1,2-diylbis(oxy)]di(ethan-1-ol) and ascribed it to these attributes. While the two adjacent ether groups common to both molecules in 2,2'-[ethane-1,2-diylbis(oxy)]di(ethan-1-ol) apparently only increased the solubility, the ring geometry in **17** might have increased the effect to a level that enabled destructive levels of interaction.

Table 4
Experimental solubilities and reference data of CL-20 in **10** and **12** at different temperatures (pressure $p = 0.1$ MPa).

Solvent	b_{CL-20}/mol • kg^{-1} published in[20]		Experimental b_{CL-20}/ mol • kg^{-1}		Δb_{CL-20}/ mol • kg^{-1}	
	273.15 /K	333.15 /K	273.15 /K	333.15 /K	273.15 /K	333.15 /K
10	1.246	1.212	1.308	1.200	0.062	-0.012
12	1.933	1.969	1.912	1.960	-0.021	-0.009

Table 3
Experimental solubilities of HMX and CL-20 in various solvents at different temperature (pressure $p = 0.1$ MPa).

Solvent	Designation	b_{HMX}/ mol • kg^{-1}		b_{CL-20}/ mol • kg^{-1}	
		293.15 /K	333.15 /K	293.15 /K	333.15 /K
Tetrahydro-2H-pyran-2-one	**2**	0.294	0.618	2.478	3.225
5-Methyloxolan-2-one	**3**	0.311	0.513	solvate	solvate
Cyclopentanone	**4**	0.101	0.155	2.207	2.385
4-Methyloxetan-2-one	**5**	0.145	0.246	2.118	2.036
Oxolane	**6**	0.014	0.020	1.433	1.511
1,3-Dioxolan-2-one	**7**	–	0.442	–	solvate
2-Oxepanone	**9**	0.463	0.685	n. d.[a]	2.054–3.195[b]
Ethyl acetate	**10**	0.010	0.017	1.308	1.200
5-Ethyloxolan-2-one	**11**	0.179	0.321	2.127	2.077
Cyclohexanone	**12**	0.088	0.172	1.912	1.960
Tetrahydrotiophene-1-oxide	**13**	1.084	1.621	solvate	n. d.
Propan-2-one	**14**	0.098	–	3.097	–
Thiophene	**15**	<0.003	<0.003	0.005	0.009
Furan	**16**	0.003	–	0.005	–
1,3-Dioxolane	**17**	0.007	0.020	solvate	solvate
4-Methyl-1,3-dioxolan-2-one	**18**	0.122	0.311	1.586	1.919
Methoxysulfinyloxymethane	**19**	0.034	0.071	1.276	1.335
N-Cyclohexyl-2-pyrrolidone	**20**	0.641	0.215	n. d.[c]	n. d.[c]
3-Methylbutyl acetate	**21**	<0.003	0.003	0.632	0.582
5-Propyloxolan-2-one	**22**	0.111	0.203	1.568	1.645
Diethyl carbonate	**23**	0.003	0.014	0.294	0.363
Ethyl methyl carbonate	**24**	0.007	0.014	0.475	0.559
Dimethyl carbonate	**25**	0.007	0.020	0.018	0.100
Tetramethylurea	**26**	0.209	0.621	2.191	2.932
Formic acid	**27**	0.003	0.007	0.014	0.030
Acetonitrile	**29**	0.071	0.165	2.848	3.131
2-Propanole	**30**	<0.003	<0.003	0.002	0.002
2-Methylpropanenitrile	**31**	0.020	0.034	1.317	1.383
Nitromethane	**32**	0.024	0.071	0.500	0.860

[a] n.d. means not determined.
[b] Extrapolated value from diluted solution due to excessive viscosity.
[c] Not determined due to excessive viscosity.

Of the tested solvents, none have shown excessive viscosities of saturated solutions of HMX. Of the tested solvents **3**, **9**, **13** and **20** have shown viscosities too high for practical application of saturated solutions of CL-20.

3.2. Solvate formation

Multiple strategies of molecular variation were pursued to identify a solvent that exhibits a similarly good solubility ratio as **1**, but does not form solvates. One strategy was to reduce the energetic benefit of solvate formation by increasing the side chain of the five-membered lactone ring. The increase in side chain length from **1** up to **22** appears to reduce the tendency of the solvent to produce solvates. While **1** forms solvates with both HMX and CL-20, for **3** only a solvate of CL-20 was observed, and no solvates were formed with **11** and **22**. The increase in side chain length corresponds with a linear decrease in solubility of HMX both at 293.15 K and 333.15 K. The CL-20 solubility however does not follow a clear trend. The reported solubility of CL-20 in **1** and the solubility of the CL-20 solvate in **3** are significantly lower that the CL-20 solubilities in **11** and **22** at 293.15 K. At 333.15 K, compared to 293.15 K the reported solubility of CL-20 in **1** and the solubility of the CL-20 solvate in **3** increase by 58% and 38%, respectively, while the solubility in **11** is unchanged and the solubility in **22** decreases compared to 293.15 K.

Another approach was to vary the lactone ring size hoping to maintain the level of interaction while reducing the energetic benefit of solvate formation. Of the three lactones with varied ring-size, none formed solvates in our solubility tests. The reported CL-20 solubility in **1** is significantly lower than the solubilities in **5**, **2** and **9**. Considering both the trends of the ring size and side chain length dependent CL-20 solubility, it appears very likely that the reported CL-20 solubility in **1** is in fact the solubility of the solvate. The solvate is necessarily less soluble than CL-20 if it is spontaneously formed in a solubility experiment. This leads to an atypically low ostensible solubility and thus to an improved perceived solubility ratio. This is similar to the situation of **7** and **3** which both exhibit a CL-20 solvate to HMX solubility ratio close to that of **1** with 2:1 and 3:1 at 333.15 K, respectively. That the reported solubility of HMX in **1** is not the solubility of the solvate is supported by the fact that even though solvates of HMX with **2**, **4**, **8**, **9**, **13** and **26** are known[39–41] these solvates did not form during our solubility tests which makes it likely that the HMX solvate of **1** also did not form in the experiments of Sitzmann et al.[24] and Svensson et al.[21] Most likely many of the HMX solvates reported are kinetic products, and their formation is in all likelihood only the result of the strong non-equilibrium conditions during their creation such as rapid cooling or fast evaporation of the solvent. It appears, for example, unlikely that HMX forms energetically beneficial solvates with a multitude of benzene and naphthalene derivates.[42]

Solvent **20** was also investigated as a more encumbered substitute for **8** to suppress solvate formation. No solvates were observed and a high HMX solubility was determined. However, no CL-20 solubility could be determined because of excessively high solution viscosity.

All of the solvates discovered in this study were formed during solubility tests. Some solvate formations took several hours under the applied conditions. It is, therefore, very likely that for some tested solvents unknown thermodynamically stable solvate of CL-20 or HMX exist. This becomes clear when one considers that **25**[43] and **29**[44] are known to form CL-20 solvates and **9**,[39] **13**,[39] **4**,[40] **8**[45] and **2**[39] are known to form HMX solvates, but no formation of solvate crystals occurred during the solubility tests.

3.3. Solubility ratio

The solubility ratios of CL-20 to HMX are displayed for 293.15 K and 333.15 K in Fig. 2. Only solvents that did not form solvates in our tests and exhibited a solubility of HMX of greater than 0.02 mol HMX per kg solvent were used for this comparison. Because of the pronounced solubility increase of HMX with increasing temperature, the solubility ratios at 333.15 K are always improved compared to 293.15 K. On average an improvement of factor 1.8 is achieved.

None of the tested solvents approaches the aimed at solubility ratio of 2:1. A solvent mixture approach was, therefore, investigated, as it has been shown for the cocrystal formers carbamazepine and saccharin that a solvent mixture for example of water and sulfolane can result in a more beneficial solubility ratio of the cocrystal formers than in both pure solvents, even though saccharin is more soluble in both solvents.[8] To investigate whether solvent mixtures can equilibrate the solubility of HMX and CL-20 too, the solubilities were determined in equimolar solvent mixtures (Tables 5 and 6). The solvents were chosen for their diversity in functional group and solubility ratio. Furthermore, **29** is known to form a CL-20 solvate and **17** has formed a CL-20 solvate in this study. Solvent mixtures should reduce the chance of solvate formation[8,46] and having solvate forming solvent in the mixture might provide additional information. As can be seen from Table 5, most solvent mixtures exhibit a solubility ratio close to the arithmetic mean of the individual solvents. Only for the mixture of **5** and **10** a solubility ratio significantly better than the mean, but still worse than the better solubility ratio, was obtained. And in the mixture of **17** and **32** a solubility value significantly worse than in **32** was observed.

These results are inconclusive; however, they also do not provide evidence for possible solubility ratio reduction by applying solvent mixtures.

These solubility data represent only one point on the mass fraction dependent solubility curve. For selected solvents, solubilities of HMX and CL-20 were, therefore, determined in varying mixtures with **30** to investigate whether a more favourable solubility ratio can be achieved depending on the solvent mixture ratio (Table 7).

No uniform behaviour of the solubility ratio depending on the mass fraction of 2-propanol in the solvent mixtures is apparent (Fig. 3), but no solvent mixture exhibits a decrease of solubility ratio within the solubility region of practical use. No further solubility tests in solvent mixtures were undertaken.

As can be seen from Fig. 2, for solvents of reasonably high solubility the solubility ratio of CL-20 and HMX can vary drastically, from 5:1 for **26** up to 42:1 for **31** at 333.15 K, but none of the tested or reported solvents possesses a HMX solubility equal or higher than that of CL-20. This speaks for inherent differences in the solvation and/or lattice enthalpy of the two substances. Because of the lack of data of the lattice enthalpy of HMX and CL-20 and the large margin of error of experimental and calculated data (the reported sublimation enthalpy data of CL-20, for example, from which one could derive the lattice enthalpy differ by over 100 $kJ \cdot mol^{-1}$)[47] no further analysis of this phenomenon was undertaken.

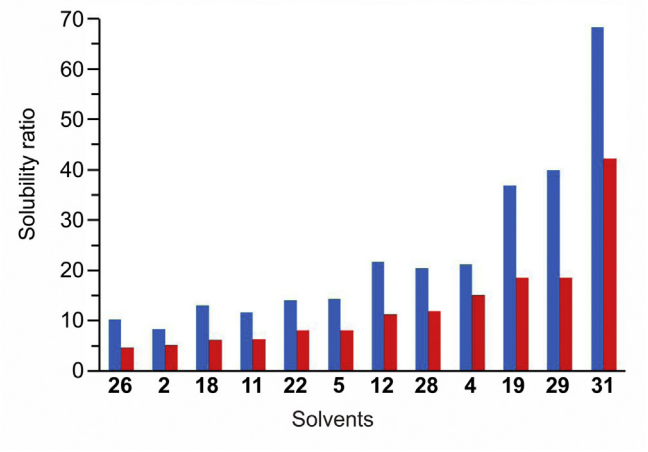

Fig. 2. Solubility ratios of CL-20 and HMX at 293.15 K (blue) and 333.15 K (red) in various solvents.

Table 5
Comparison of the solubility ratios of CL-20 and HMX in equimolar solvent mixtures with the arithmetic mean and the solubility ratio of CL-20 and HMX in the pure solvents.

Solvent A	Solvent B	Solubility ratio of solvent A	Solubility ratio of solvent B	Arithmetic mean	Obtained solubility ratio
5	**10**	8	71	40	17
17	**5**	n.d.[a]	8	–	13
17	**32**	n.d.[a]	12	–	24
29	**10**	19	71	45	34
29	**32**	19	12	15	15

[a] No solubility ratio of **17** was determinable because of solvate formation.

Table 6
Experimental solubilities of HMX and CL-20 in equimolar solvent mixtures at 333.15 K and 0.1 MPa.

Solvent A	Solvent B	b_{HMX}/ mol • kg^{-1}	b_{CL-20}/ mol • kg^{-1}
5	**10**	0.093	1.578
17	**5**	0.140	1.816
17	**32**	0.045	1.102
29	**10**	0.051	1.750
29	**32**	0.110	1.684

3.4. Solvent selection for cocrystallisation

Considering the abundance of solvate forming solvents, that often solvents either form HMX or CL-20 solvates, that for eight of the ten best solvents for HMX solvates are known, and that some tested solvents might possess undiscovered solvates, the strict exclusion of solvate forming solvents from consideration for CL-20/HMX-cocrystal generation needs to be revaluated. It is proposed that the possible formation of thermodynamic stable HMX solvates in general constitutes a far greater hindrance to the formation of the cocrystal than a possible CL-20 solvate formation because one would most likely operate a cocrystallisation for efficiency reasons close to the HMX/cocrystal phase boundary in the ternary phase diagram which is most likely the phase region of the HMX solvate phase. A solution composition for crystallisation close to the HMX phase boundary seems reasonable because all tested, and possibly all solvents in general, exhibit a far worse solubility ratio than 2:1 in the tested temperature range. Even solvents that spontaneously produce CL-20 solvate can, therefore, be considered for cocrystallisation. It is very

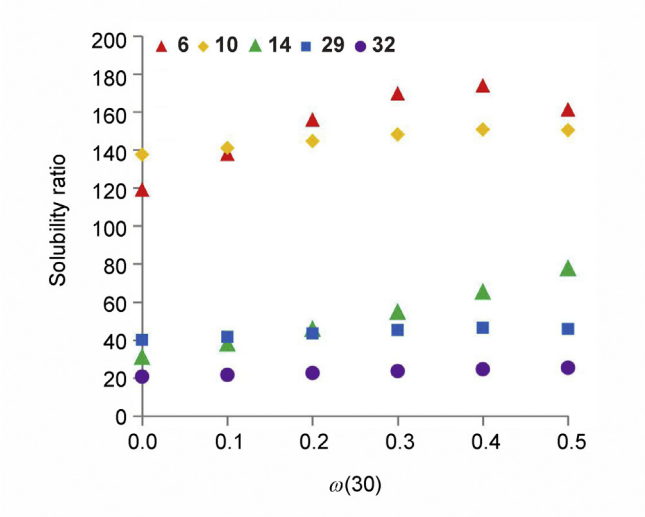

Fig. 3. Solubility ratio progression of CL-20 and HMX in various solvent mixtures with **30**. Red triangles **6**, yellow rhombs **10**, green triangles **14**, blue squares **29**, violet circles **32**.

Table 7
Experimental molalities *b* of CL-20 and HMX in mixtures of liquid solvent with **30** of mass fraction *w* at 293.15 K and 0.1 MPa.

Solvent	w_{30}	b_{CL-20}/mol • kg^{-1}	w_{30}	b_{HMX}/mol • kg^{-1}	Solvent	w_{30}	b_{CL-20}/mol • kg^{-1}	w_{30}	b_{HMX}/mol • kg^{-1}
6	1	0.002	1	0.000	**29**	0.9318	0.011	0.9289	0.001
	0.8796	0.015	0.8822	0.001		0.8525	0.044	0.8538	0.002
	0.7696	0.056	0.769	0.001		0.772	0.110	0.7727	0.002
	0.6608	0.144	0.6587	0.001		0.6883	0.222	0.6868	0.006
	0.5498	0.316	0.5547	0.002		0.5907	0.410	0.5931	0.009
	0.4584	0.499	0.4546	0.003		0.4911	0.642	0.4943	0.015
	0.3667	0.683	0.3579	0.004		0.3909	1.016	0.3861	0.023
	0.2656	0.897	0.2627	0.006		0.2715	1.477	0.2663	0.031
	0.1683	1.171	0.1715	0.007		0.1382	2.146	0.1408	0.051
	0.0833	1.316	0.0843	0.009		0	2.848	0	0.071
	0	1.511	0	0.013					
					32	0.8967	0.005	0.8947	0.001
10	0.8604	0.018	0.8591	0.001		0.7912	0.016	0.7972	0.001
	0.7316	0.071	0.7326	0.001		0.6331	0.054	0.6913	0.002
	0.6162	0.163	0.6144	0.001		0.5896	0.071	0.5953	0.003
	0.5083	0.292	0.5061	0.002		0.4961	0.115	0.4955	0.004
	0.4014	0.455	0.4067	0.003		0.3952	0.175	0.3954	0.007
	0.3109	0.621	0.3142	0.004		0.2955	0.250	0.2968	0.010
	0.224	0.812	0.2258	0.005		0.1978	0.323	0.177	0.016
	0.1409	0.966	0.1448	0.006		0.098	0.432	0.0985	0.020
	0.0704	1.213	0.0715	0.008		0	0.499	0	0.024
	0	1.308	0	0.009					
14	0.9032	0.023	0.9023	0.000					
	0.7918	0.108	0.8048	0.001					
	0.7065	0.184	0.7062	0.002					
	0.6084	0.483	0.6068	0.005					
	0.5107	0.715	0.5097	0.010					
	0.4105	1.224	0.4069	0.018					
	0.3086	1.633	0.307	0.029					
	0.1971	2.285	0.2073	0.046					
	0.0975	2.630	0.104	0.069					
	0	3.097	0	0.098					

likely that many of the reported solvates of HMX are kinetic products that would hence possess a higher solubility than pure HMX. These kinds of solvates would most likely not disturb the cocrystallisation process, and these solvents are most likely suited for consideration for cocrystallisation. Because CL-20 is in all solvents far more soluble than HMX, it appears that the most promising candidates for consideration as solvent for solution based cocrystallisation of CL-20 and HMX are the solvents exhibiting the best solubility ratio that do not form thermodynamically stable HMX solvates. Based on these findings, for the solvents that exhibited the best solubility ratios, cocrystallisation tests have been carried out and published.[7] Absolute solubility, chemical compatibility, and crystal morphology narrowed the selection down to **29** in these tests.[7] Because of the temperature dependency of the HMX solubility, high-boiling solvents might be of special interest for further crystallisation experiments, as at even higher temperatures than 333.15 K better solubility ratios should be achievable and other solvents than **29** might become viable.

3.5. Solvate characterisation

Solvents **3**, **7**, **13**, **17**, **28** and **33** have formed solvates with CL-20 in our solubility tests. Except for the **28** solvate, for all solvates single crystals suited for x-ray structural analysis were obtained. As can be seen from Fig. 4, where the normalised mass loss over time is displayed for the solvate crystals under atmospheric conditions, aside from the solvate of **7** none of the solvates are stable under atmospheric conditions. The **17** solvate reached total desolvation the fastest with 116 h followed by the **28** and **33** solvates with 166 h. Between 1031 and 6600 h, the **3** solvate reached total desolvation, while the **13** solvate still retains a vestige amount of solvent after 6600 h.

Because of the instability of the solvates, no pure material aside from the individual crystals for single crystal structure determination could be obtained. Further analysis was carried out with fresh solvate material that was washed following the standard washing procedure and dried quickly to minimise the desolvation. The solvate of **13** desolvated completely during the washing. To obtain samples for analysis, this material was then only dried on filter paper to remove most of the adherent solution. Raman spectra, DSC diagrams, and TGA diagrams of the washed samples are found in the supporting information.

Even though all solvates dissociate at room temperature except for the **7** solvate, during TGA analysis sharp desolvation temperatures significantly higher than room temperature were determined (Table 8). The two-step mass loss of the **3** solvate during the TGA starting at a very mild 308 K but proceeding stronger between 335 K and 367 K correlates well with the initial rapid mass loss at atmospheric conditions and the following slower mass loss. The **7** solvate also exhibits a two-step mass loss that correlates well with two distinct endothermic signals in the DSC diagram (Table 9). All solvates except for the **13** solvate exhibit a typically broad endothermic signal in the DSC measurement 14–72 K higher that the desolvation onset in the TGA. This is attributed to the desolvation and evaporation of the solvent. The **13** solvate, however, exhibits an endothermic signal 20 K lower than the desolvation onset which could indicate a phase change before desolvation occurred. The **13** solvate, furthermore, is the only compound that exhibits a significantly lower decomposition temperature both in the TGA and DSC measurement than pure CL-20. The comparison of the temperature dependent mass loss curves (Figure S13) show that evaporation of solvent and decomposition of CL-20 fade into each other only for the **13** solvate.

The single crystal data of the five novel solvates of CL-20 are discussed in the following, and the crystallographic informations are displayed in Table 10.

In the crystal structure (orthorhombic, $P2_12_12$) of CL-20:**33**, there is one and a half independent **33** present for every independent CL-20. The "halve" **33** is situated on the border of the asymmetric unit acting as an inversion centre. This molecule is disordered about its position in the crystal lattice and its contact is limited to four weak O· · · H – C

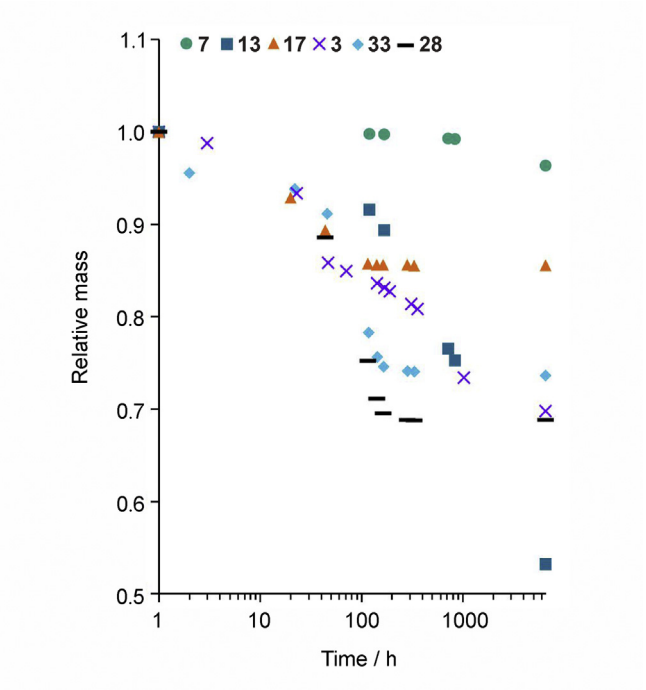

Fig. 4. Mass loss of the solvates at 293 K and 0.1 hPa. With the CL-20 solvates of **7** in green circles, **13** in blue squares, **17** in orange triangles, **3** in violet crosses, **33** in teal diamonds and **28** in black dashes.

Table 8
Desolvation onsets during the TGA of the solvates.

	First desolvation onset /K	Second desolvation onset /K
3	308	333
28	311	–
17	319	–
33	325	–
13	345	–
7	371	423

Table 9
Endothermic heat flow during the DSC analysis of the solvates.

Solvates	First endothermic peak (max heat flow) /K	Second endothermic peak (max heat flow) /K
13	326	–
17	341	–
28	359	–
33	361	–
3	380	–
7	418	445

interactions (ca. 2.5–2.6 Å) with two adjacent CL-20. Hence, no significant interaction between the two independent **33** molecules is present. CL-20, assuming the conformation found in γ-CL-20, forms a zig-zag chain of strong O · · · H – C interactions (2.3 Å) along the b-axis in which each molecule is related to the next by inversion symmetry. The **33** are bound to this chain on alternating sides by moderate O · · · H – C interactions (ca. 2.4 Å). These chains form a layer structure in the bc-plane, which is linked in c direction only by weak O · · · H – C interactions (2.6 Å) between CL-20 molecules.

The conformation found in γ-CL-20 is also observed in the crystal structure (monoclinic, *Cc*) of CL-20: **7**, where four independent CL-20 and four independent **7** are present in the asymmetric unit. Two of the CL-20 possess two strong O · · · H – C interactions (2.2 Å) each. Of the independent **7** molecules, three possess each two to three moderate O · ·

Table 10
Crystallographic information for the five CL-20 solvates.

Parameters	**3**	**7**	**13**	**17**	**33**
Space group	$P\bar{1}$	*Cc*	$P2_1/c$	$P2_1/c$	$P2_12_12$
Crystal system	Triclinic	Monoclinic	Monoclinic	Monoclinic	Orthorhombic
a/Å	7.1967(7)	15.8685(5)	12.6725(4)	8.9577(3)	21.5458(8)
b/Å	12.1864(10)	20.1229(6)	33.1797(16)	12.6281(4)	12.5600(5)
c/ Å	15.9929(16)	22.9923(8)	18.0049(6)	15.6248(6)	8.0755(3)
α/°	100.573(7)	90	90	90	90
β/°	102.412(8)	90.246(3)	92.411(3)	96.746(4)	90
γ/°	106.818(8)	90	90	90	90
V/ Å^3	1265.1(5)	7341.8(4)	7563.8(5)	1755.2(2)	2185.3(5)
Z	2	16	4	4	4
ρ/g·cm^{-3}	1.676	1.905	1.593	1.939	1.724
T/K	110	110	293	115	113
Stoichiometry	1:2	1:1	2:9	1:1	2:3
Chemical Formula	$C_6H_6N_{12}O_{12}$: $2C_5H_8O_2$	$C_6H_6N_{12}O_{12}$: $C_3H_4O_3$	$2C_6H_6N_{12}O_{12}$: $9C_4H_8OS$	$C_6H_6N_{12}O_{12}$: $C_3H_6O_2$	$2C_6H_6N_{12}O_{12}$: $3C_4H_6O_2$
CL-20 conformation	*ε*	*γ*	*ξ* + *ϑ*	*ε*	*γ*
R_1	0.057	0.0401	0.0667	0.0286	0.031
CCDC	2049488	2049491	2049489	2049492	2049490

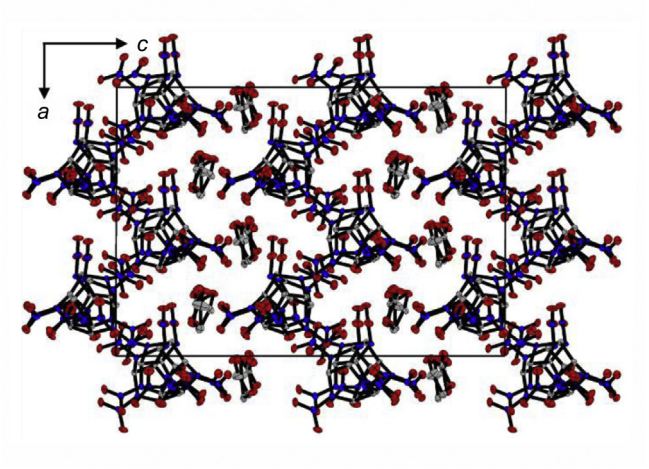

Fig. 5. The layered arrangement observed in CL-20:**7**. Hydrogens are omitted for clarity.

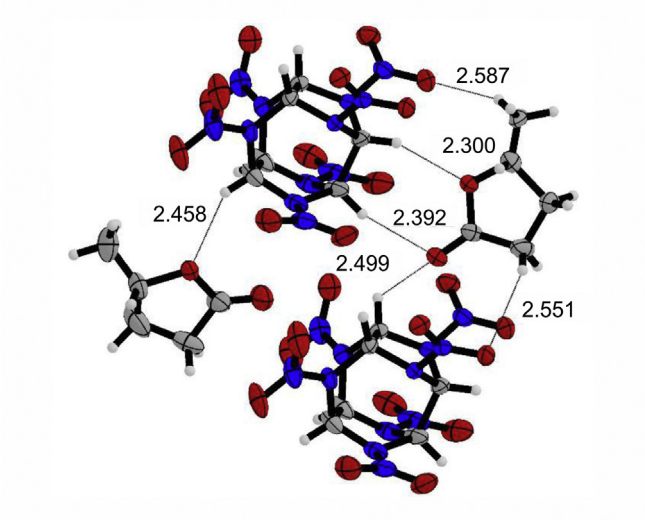

Fig. 6. The intermolecular O···H – C interactions between CL-20 and the two independent molecules of **3**. Contact length is displayed in Å. Only contacts of less than VdW radius - 0.1 Å are displayed. One interaction of length 2.6 Å is omitted for both positions for clarity reasons. Thermal ellipsoids are set to 50% probability.

·H – C interactions (ca. 2.3–2.4 Å), while the other **7** only exhibits weak O···H – C interactions (ca. 2.5–2.6 Å). This might explain the two-step mass loss during the TGA. The molecules are arranged in alternating single stack zig-zag layer in the ab-plane (Fig. 5).

CL-20: **3** (in a 1:2 ratio) has been found to crystallise in the triclinic crystal system ($P\bar{1}$), in which CL-20 exhibits the conformation found in *ε*-CL-20. Because of the chirality of **7**, two independent **7** are present in the unit cell. Both positions, however, are disordered, as at both positions both enantiomers can be found in the crystal. From Fig. 6 it can also be seen that one position exhibits significantly stronger interactions than the other. This asymmetry is most likely the reason for the two-stage desolvation observed during the TGA.

The layered nature of the overall structure becomes evident when viewed down the *a*-axis (Fig. 7). **3** is arranged in a zig-zag layer while CL-20 is arranged in a flat plane.

The conformation found in *ε*-CL-20 is also observed in the crystal structure (monoclinic, $P2_1/c$) of CL-20:**17**. CL-20 and **17** form an alternating layer system in the ab-plane that is connected in three dimensions with moderately weak O···H – C interactions (ca. 2.4–2.5 Å). **17** acts as the donor in the strongest O···H – C interactions (2.38 Å). No short contact exists between the oxygens of **17** and the nitramine groups of CL-20. This indicates that the destabilising interaction observed in solution is most likely not present in the crystal structure. A destabilising interaction of the acetal group's oxygen lone pairs with the σ^* orbital of the nitramine group might cause the decomposition in solution. As the σ^* orbitals of the N-N-bonds extend from CL-20 in line with the bonds themselves, solvent **17** would need to be positioned in extension of the N-N-bonds. From Fig. 8 it can be seen, however, that **17** is situated between the nitramine groups. No significant interaction of the oxygen lone pairs of **17** with the σ^* orbitals of the N-N-bonds is, therefore, possible.

The CL-20:**13** solvate's crystal structure (monoclinic, $P2_1/c$) is formed by two independent CL-20 molecules and nine independent **13** molecules of which one is disordered. This structure comprises clusters of four CL-20 situated over inversion centre that are isolated from each other by a layer of **13** (Fig. 9). **13** therefore forms a 3 D net throughout the crystal. The nine independent molecules of **13** all exhibit different levels of O···H – C interactions ranging from one to four interactions and 2.2 up to 2.6 Å. The weakest bonded **13** only possesses one moderate interaction (2.4 Å). The difference in intermolecular bonding strength of all nine **13** explains the wide temperature range over which desolvation occurred in the TGA. One of the independent CL-20 adopts the conformation found in ξ-CL-20. This conformation has previously only been found in two additional crystal structures aside from ξ-CL-20.[48,49] The

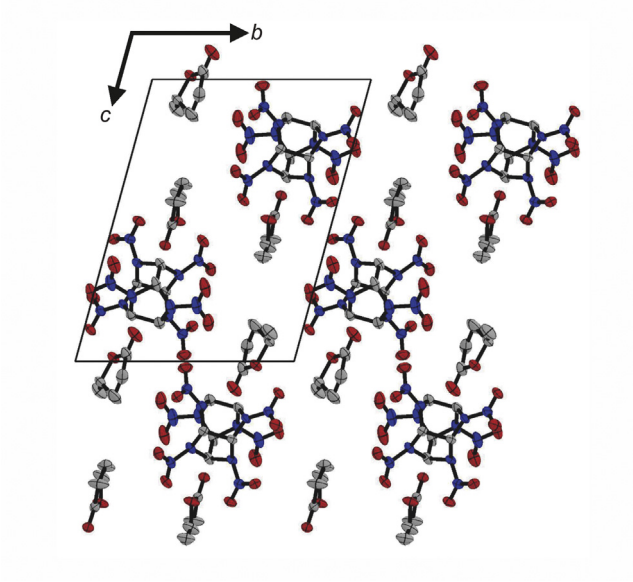

Fig. 7. The layered arrangement observed in CL-20:**3**. Hydrogens are omitted for clarity. Thermal ellipsoids are set to 50% probability.

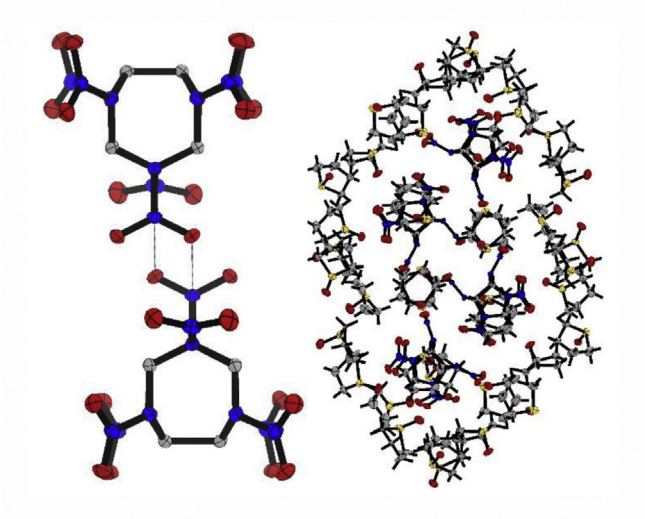

Fig. 9. N···O interaction between CL-20 forming an inversion centre (left). Hydrogens are omitted for clarity. Thermal ellipsoids are set to 50% probability. Visualisation of the enveloping cluster of **13** around the four CL-20 around the inversion centre.

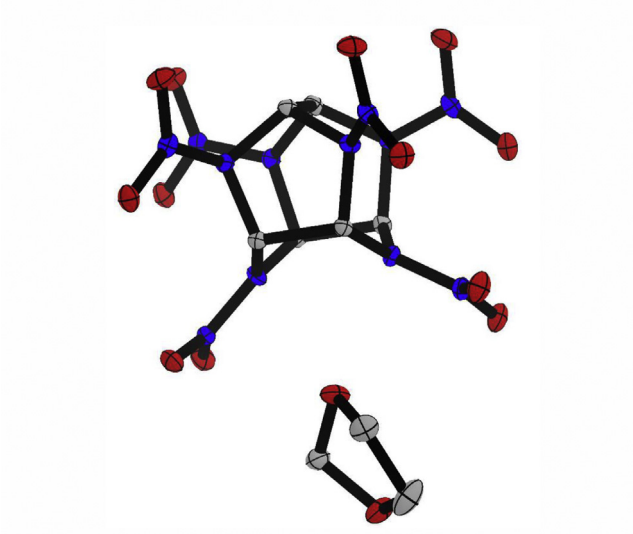

Fig. 8. Visualisation of the lack of strong interaction between the acetal group of **17** and the nitramine groups of CL-20. Hydrogens are omitted for clarity. Thermal ellipsoids are set to 50% probability.

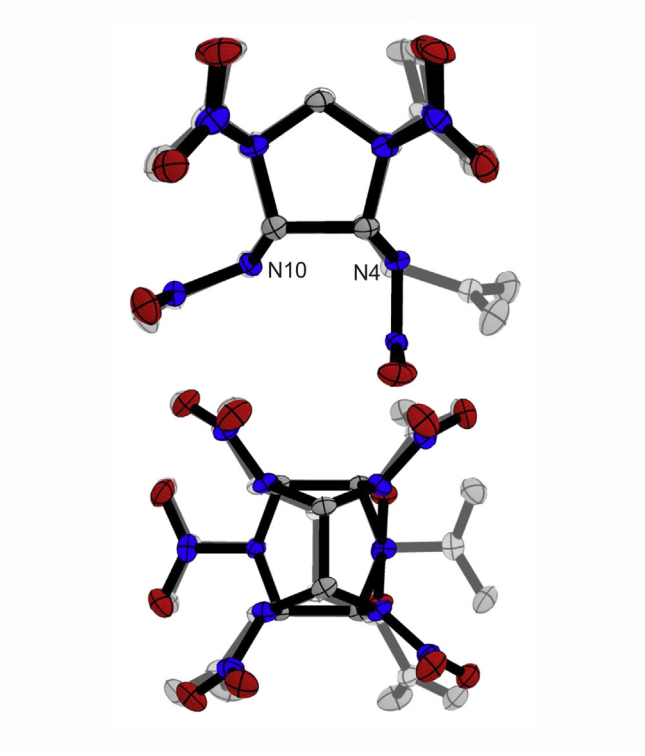

Fig. 10. Superposition of the two independent CL-20 in the CL-20:**13** solvate displayed from two angles. The molecule that adopts the conformation found in ξ-CL-20 is displayed in grey. Thermal ellipsoids are set to 50% probability. Hydrogens are omitted for clarity.

other CL-20 in the crystal structure of the CL-20:***13*** solvate crystal, however, exhibits a conformation (Fig. 10) that was believed to be sterically unfavourable[50,51] and has never previously been described. Hence, a novel ϑ-conformation was discovered. The conformation is similar to the conformation of CL-20 in the ξ phase, but the nitramine group situated at N4 (Fig. 10) is in endo position. The resulting lone pair repulsion seems to be mitigated by the quite severe out-of-plane bend angle (44°) of the nitramine group relative to the six-membered ring plane (Fig. 10). Only two other CL-20 conformation are known to date that exhibits an endo orientation of N4 or N10: ε-CL-20 and η-CL-20.[52] The solvate's crystal structure gives no obvious indications why this highly unusual conformation occurs. The CL-20 in question possesses O···N interactions with an inversion symmetrical CL-20 (Fig. 5). This interaction is weak (2 × 3.1 Å) compared to similar interactions found in ε-CL-20 (2.8 and 3.1 Å) and ξ-CL-20 (2 × 2.6 Å). This interaction is, therefore, most likely not responsible for the unusual conformation and the unusually low decomposition temperature of the solvate. During research concerning the novelty of the ϑ-conformation, five CL-20 containing cocrystals were found that all seem to contain CL-20 in an also undescribed conformation.[52–55] The conformation closely resembles ε-CL-20. Here, however, the six-ring nitramine groups both exhibit exo orientation (Fig. 11) instead of endo-exo orientation found in ε-CL-20.[50]

Fig. 11. Superposition of the undescribed CL-20 conformations with the conformation found in ε-CL-20 (black). Hydrogens are omitted for clarity.

While the nitramine group at N4 is endo bent by 2° in ε-CL-20, the nitramine groups at N4 are bent between 14° and 25° exo in the undescribed conformation. The first crystal containing this conformation was, to the best of our knowledge, published by Urbelis, Young, and Swift in 2015.[55]

4. Conclusion

The solubility of CL-20 and HMX was determined in 29 solvents at 293.15 K and 333.15 K and 5 ternary mixtures at 293.15 K. The strong temperature dependency of the HMX solubility was confirmed and a, for the most parts, temperature independence of the CL-20 solubility was found. Furthermore, it was found that HMX is always far less soluble than CL-20 with a solubility ratio ranging from 5:1 for **26** at 333.15 K up to 210:1 for **21** at 293.15 K. Solubility ratios that appeared to be closer to 2 were only found when a CL-20 solvate was formed. Because of the abundance of reported solvate forming solvents and the unfavourable solubility ratio it is proposed that for cocrystallisation of the CL-20/HMX cocrystal only solvents that form thermodynamic stable HMX solvates might be excluded from consideration. The analysis of the five obtained crystal structures of the six new solvates of CL-20 revealed a novel CL-20 conformation that is thought to be energetically unfavourable but might provide further insight into the potential energy surface of the CL-20 conformations.

Declaration of competing interest

The authors declare that they have no known competing financial interests or personal relationships that could have appeared to influence the work reported in this paper.

Acknowledgment

We are grateful for financial support provided by the German Ministry of Defence and the support provided by Dr. Manfred Kaiser and Dr. Michael Koch at the WTD91.

Appendix A. Supplementary data

Supplementary data to this article can be found online at https://doi.org/10.1016/j.enmf.2021.01.004.

References

1. Bolton O, Simke LR, Pagoria PF, Matzger AJ. High power explosive with good sensitivity: A 2:1 cocrystal of CL-20:HMX. *Crys Growth Des*. 2012;12(9):4311–4314.
2. An C, Li H, Ye B, Wang J. Nano-CL-20/HMX cocrystal explosive for significantly reduced mechanical sensitivity. *J Nanomater*. 2017;2017(5):1–7.
3. Anderson SR, am Ende DJ, Salan JS, Samuels P. Preparation of an energetic-energetic cocrystal using resonant acoustic mixing. *Propellants, Explos Pyrotech*. 2014;39(5):637–640.
4. Qiu H, Patel RB, Damavarapu RS, Stepanov V. Nanoscale 2CL-20·HMX high explosive cocrystal synthesized by bead milling. *CrystEngComm*. 2015;17(22):4080–4083.
5. Sun S, Zhang H, Liu Y, Xu J, Huang S, Wang S, et al. Transitions from separately crystallized CL-20 and HMX to CL-20/HMX cocrystal based on solvent media. *Cryst Growth Des*. 2018;18(1):77–84.
6. Ghosh M, Sikder AK, Banerjee S, Gonnade RG. Studies on CL-20/HMX (2:1) cocrystal: A new preparation method and structural and thermokinetic analysis. *Cryst Growth Des*. 2018;18(7):3781–3793.
7. Herrmannsdörfer D, Gerber P, Heintz T, Herrmann MJ, Klapötke TM. Investigation of crystallisation conditions to produce CL-20/HMX cocrystal for polymer-bonded explosives. *Propellants, Explos Pyrotech*. 2019;44(6):668–678.
8. Rager T, Hilfiker R. Cocrystal formation from solvent mixtures. *Cryst Growth Des*. 2010;10(7):3237–3241.
9. *CrysAlisPro: Oxford Diffraction Ltd*. Oxford Diffraction Ltd; 2009.
10. Altomare A, Cascarano G, Giacovazzo C, Guagliardi A. SIR-92, A program for crystal structure solution. *J Appl Crystallogr*. 1993;26:343.
11. Altomare A, Burla MC, Camalli M, Cascarano G, Giacovazzo C, Guagliardi A, et al. *J Appl Crystallogr*. 1999;32:115–119.
12. Altomare A, Cascarano G, Giacovazzo C, Guagliardi A, Moliterni AGG, Burla MC, et al. *SIR97, Program for Solving and Refining Crystal Structures*. 1997.
13. Sheldrick GM. *Acta Crystallogr, Sect A*. 2008;64:112–122.
14. Sheldrick GM. *SHELX-97*. University of Göttingen; 1997.
15. Spek A, Platon L. *A Multipurpose Crystallographic Tool*. Utrecht University; 1999.
16. *SCALE3 ABSPACK – An Oxford Diffraction Program*. Oxford Diffraction Ltd; 2005.
17. von Holtz E, Ornellas D, Foltz MF, Clarkson JE. The solubility of epsilon-CL-20 in selected materials. *Propellants, Explos Pyrotech*. 1994;19(4):206–212.
18. Zimmerman JHK. The experimental determination of solubilities. *Chem Rev*. 1952;51(1):25–65.
19. Internal Report.
20. Cui C, Ren H, Huang Y, Jiao Q. Solubility measurement and correlation for ε-2,4,6,8,10,12-Hexanitro-2,4,6,8,10,12-hexaazaisowurtzitane in five organic solvents at temperatures between 283.15 and 333.15 K and different chloralkane + ethyl acetate binary solvents at temperatures between 283.15 and 323.15 K. *J Chem Eng Data*. 2017;62(4):1204–1213.
21. Svensson L, Nyqvist J-O, Westling L. Crystallization of HMX from γ-butyrolactone. *J Hazard Mater*. 1986;13(1):103–108.
22. Fuhr I, Mikonsaari I. In: *Production and Characterization of Insensitive Explosive*. 2004.
23. Gibbs TR, Popolato A, eds. *LASL Explosive Property Data*. Berkeley, Calif: Univ. of Calif. Pr; 1980.
24. Sitzmann ME, Foti S, Misener CC. *Solubilities of High-explosives: Removal of High Explosive Fillers from Munitions by Chemical Dissolution*. Maryland: White Oak; 1973.
25. Internal Report.
26. Good DJ, Rodríguez-Hornedo N. Solubility advantage of pharmaceutical cocrystals. *Cryst Growth Des*. 2009;9(5):2252–2264.
27. van der Heijden AEDM, Bouma RHB. Crystallization and characterization of RDX, HMX, and CL-20. *Cryst Growth Des*. 2004;4(5):999–1007.
28. Millar DIA, Maynard Casely HE, Allan DR, Cumming AS, Lennie AR, Mackay AJ, et al. Crystal engineering of energetic materials: Co-crystals of CL-20. *CrystEngComm*. 2012;14(10):3742.
29. Aitipamula S, Banerjee R, Bansal AK, Biradha K, Cheney ML, Choudhury AR, et al. Polymorphs, salts, and cocrystals: What's in a name? *Cryst Growth Des*. 2012;12(5):2147–2152.
30. Bond AD. What is a co-crystal? *CrystEngComm*. 2007;9(9):833.
31. Desiraju GR. Crystal and co-crystal. *CrystEngComm*. 2003;5(82):466.
32. Stahly GP. Diversity in single- and multiple-component crystals. The search for and prevalence of polymorphs and cocrystals. *Cryst Growth Des*. 2007;7(6):1007–1026.
33. Blom CE, Günthard HH. Rotational isomerism in methyl formate and methyl acetate; a low-temperature matrix infrared study using thermal molecular beams. *Chem Phys Lett*. 1981;84(2):267–271.
34. Wennerstrom H, Forsen S, Roos B. Ester group. I. Ab initio calculations on methyl formate. *J Phys Chem*. 1972;76(17):2430–2436.
35. Wang X, Houk KN. Theoretical elucidation of the origin of the anomalously high acidity of Meldrum's acid. *J Am Chem Soc*. 1988;110(6):1870–1872.
36. Thome V. *Computer Simulationen als Hilfsmittel zur Kristallisation polymorpher organischer Substanzen am Beispiel von HNIW Heidelberg*. thesis. 2004.
37. Philip Thomas, Cook Robert L, Malloy Jr Thomas B, Allinger Norman L, Chang Scott, Yuh Young. Molecular mechanics calculations and experimental studies of conformations of.delta.-valerolactone. *J Am Chem Soc*. 1981;103(9):2151–2156.
38. SNPE safety data sheet of CL-20.
39. Selig W. New adducts of octahydro-1,3,5,7-tetranitro-1,3,5,7-tetrazocine (HMX). *Propellants, Explos Pyrotech*. 1982;7(3):70–77.
40. George RS, Cady HH, Rogers RN, Rohwer RK. Solvates of octahydro-1,3,5,7-tetranitro- 1,3,5,7- tetrazocine (HMX). Relatively stable monosolvates. *Ind Eng Chem Prod Res Dev*. 1965;4(3):209–214.
41. Selig W. *Some 1:1 complexes of cyclomethylenetetranitramine (HMX) and their application to the estimation of HMX in admixture with RDX*. 1964.
42. Selig W. Adducts of 1,3,5,7-tetranitro-1,3,5,7-tetraazacyclooctane (HMX). *Explosivstoffe*. 1969;17(4):73–86.
43. Shen F. The pseudosymmetric crystal structure of 2,4,6,8,10,12-hexanitrohexaazaisowurtzitane dimethyl carbonate (2/3), C21H30N24O33. *Z Kristallogr N Cryst Struct*. 2019;234(3):387–389.

44. Pan B, Dang L, Wang Z, Jiang J, Wei H. Preparation, crystal structure and solution-mediated phase transformation of a novel solid-state form of CL-20. *CrystEngComm*. 2018;20(11):1553–1563.
45. Haller TM, Rheingold AL, Brill TB. Structure of the 1/1 complex between octahydro-1,3,5,7-tetranitro-1,3,5,7-tetrazocine (HMX), C4H8N8O8, and N-methyl-2-pyrrolidinone (NMP), C5H9NO. *Acta Crystallogr C Cryst Struct Commun*. 1985;41(6):963–965.
46. Sun X, Yin Q, Ding S, Shen Z, Bao Y, Gong J, et al. (Solid + liquid) phase diagram for (indomethacin + nicotinamide)-methanol or methanol/ethyl acetate mixture and solubility behavior of 1:1 (indomethacin + nicotinamide) co-crystal at T=(298.15 and 313.15) K. *J Chem Therm*. 2015;85:171–177.
47. Dorofeeva OV, Suntsova MA. Enthalpy of formation of CL-20. *Comput Theor Chem*. 2015;1057:54–59.
48. Aldoshin SM, Aliev ZG, Goncharov TK, Korchagin DV, Milekhin YM, Shishov NI. New conformer of 2,4,6,8,10,12-hexanitro-2,4,6,8,10,12-hexaazaisowurtzitane (CL-20). Crystal and molecular structures of the CL-20 solvate with glyceryl triacetate. *Russ Chem Bull*. 2011;60(7):1394–1400.
49. Zyuzin IN, Aliev ZG, Goncharov TK, Ignatieva EL, Aldoshin SM. Structure of a bimolecular crystal of 2,4,6,8,10,12-hexanitro-2,4,6,8,10,12-hexaazaisowurtzitane and methoxy-NNO-azoxymethane. *J Struct Chem*. 2017;58(1):113–118.
50. Foltz MF, Coon CL, Garcia F, Nichols AL. The thermal stability of the polymorphs of hexanitrohexaazaisowurtzitane, Part I. *Propellants, Explos, Pyrotech*. 1994;19(1):19–25.
51. Sysolyatin SV, Lobanova AA, Chernikova YT, Sakovich GV. Methods of synthesis and properties of hexanitrohexaazaisowurtzitane. *Russ Chem Rev*. 2005;74(8):757–764.
52. Aliev ZG, Goncharov TK, Dashko DV, Ignat'eva EL, Vasil'eva AA, Shishov NI, et al. Polymorphism of bimolecular crystals of CL-20 with tris[1,2,5]oxadiazolo[3,4-b:3',4'-d:3″,4″-f]azepine-7-amine. *Russ Chem Bull*. 2017;66(4):694–701.
53. Tan Y, Yang Z, Wang H, Li H, Nie F, Liu Y, et al. High energy explosive with low sensitivity: A new energetic cocrystal based on CL-20 and 1,4-DNI. *Cryst Growth Des*. 2019;19(8):4476–4482.
54. Yang Z, Wang H, Ma Y, Huang Q, Zhang J, Nie F, et al. Isomeric cocrystals of CL-20: A promising strategy for development of high-performance explosives. *Cryst Growth Des*. 2018;18(11):6399–6403.
55. Urbelis JH, Young VG, Swift JA. Using solvent effects to guide the design of a CL-20 cocrystal. *CrystEngComm*. 2015;17(7):1564–1568.

Dirk Herrmannsdörfer received his M.Sc. in Chemistry from University Stuttgart in 2013. His fields of study focused on physical chemistry (bachelor thesis), element organic chemistry (master thesis) and theoretical chemistry (master program). He is working at Fraunhofer-Institute for Chemical Technology since 2014 where he has developed the scaled-up production of high-quality CL-20/HMX cocrystal. Since 2015, he is working on his Ph. D. under the supervision of Professor Klapötke of the Ludwig-Maximilians University of Munich. His current research interests include online infrared spectroscopy, helium pycnometry, technical chemistry, crystallisation, and chemometrics.